International Journal of Minerals, Metallurgy and Materials
Volume 25, Number 3, March 2018, Page 310
https://doi.org/10.1007/s12613-018-1574-y

Solid-phase synthesis of Cu_2MoS_4 nanoparticles for degradation of methyl blue under a halogen-tungsten lamp

Shi-na Li[1)], *Rui-xin Ma*[1,2)], *and Cheng-yan Wang*[1)]

1) School of Metallurgical and Ecological Engineering, University of Science and Technology Beijing, Beijing 100083, China
2) Beijing Key Laboratory of Special Melting and Preparation of High-End Metal Materials, Beijing 100083, China
(Received: 18 May 2017; revised: 6 November 2017; accepted: 7 November 2017)

Abstract: The Cu_2MoS_4 nanoparticles were prepared using a relatively simple and convenient solid-phase process, which was applied for the first time. The crystalline structure, morphology, and optical properties of Cu_2MoS_4 nanoparticles were characterized using X-ray diffraction, X-ray photoelectron spectroscopy, field emission scanning electron microscopy, and UV-vis spectrophotometry. Cu_2MoS_4 nanoparticles having a band gap of 1.66 eV exhibits good photocatalytic activity in the degradation of methylene blue, which indicates that this simple process may be critical to facilitate the cheap production of photocatalysts.

Keywords: Cu_2MoS_4 nanoparticles; solid-phase synthesis; degradation; photocatalyst; methyl blue

1. Introduction

Recently, semiconductor photocatalysts have attracted considerable research attention to be applied to degrade organic pollutants and to produce hydrogen by water splitting [1–7]. Among various semiconductor photocatalysts, transition metal sulfides (TMSs) and Cu_2MX_4 (M = Mo or W and X = S or Se) are considered to be ideal because of their excellent light absorption in the visible region [8–10]. Cu_2MoS_4 is a typical TMS that possesses excellent photocatalytic activity and may even be better than some high-cost noble-metal photocatalysts [11–13]. Cu_2MoS_4 has two structural phases, one allotrope of which is in the $P\bar{4}2m$ space group and another is in the $I42m$ space group, which makes it similar to Cu_2WS_4 [14]. The primary synthesizing method for Cu_2MoS_4 is a hydrothermal method. Crossland *et al.* [15] reported the synthesis of Cu_2MoS_4 by a solvothermal method employing $(Cu(CH_3CN))(BF_4)$ and $(NH_4)_2(MoS_4)$ at 110–150°C for 48 h. Further, Liang *et al.* [16], Jing *et al.* [17], and Tran *et al.* [18] used a hydrothermal method to prepare a crystalline Cu_2MoS_4 photocatalyst that exhibited good photocatalytic activity. Zhang *et al.* [19] used various initial reactants to synthesize Cu_2MoS_4 through a hydrothermal method, which resulted in a product having excellent photocatalytic activity, good recycling performance, and durability in the degradation of methyl orange (MO) dye under visible-light irradiation. Recently, the indented nanosheets of I-Cu_2MoS_4 was synthesized using Cu_2MoS_4 flat nanosheets templates, and this product exhibited good photocatalytic activity for the degradation of Rhodamine B within 90 min [20].

In this study, a simple solid-phase process was used to synthesize Cu_2MoS_4 nanoparticles to produce low-cost photocatalysts at 200°C in the presence of air. Compared to the liquid-phase processes such as the solvothermal method, the solid-phase process is considered to be more environment-friendly, cheap, and simple. It is worth noting that this process can also be applied to synthesize other Cu-based sulfide materials, as detailed in our previous reports [21]. However, no studies have been conducted on this method until now, to the best of our knowledge. The prepared Cu_2MoS_4 material exhibits good photocatalytic performance in the photodegradation of methylene blue (MB), under irradiation using a low-power (300 W) halogen-tungsten lamp.

Corresponding author: Rui-xin Ma E-mail: maruixin@ustb.edu.cn; Cheng-yan Wang E-mail: wchy3207@sina.com

2. Experimental

2.1. Synthesis of Cu_2MoS_4 nanoparticles using a solid-phase process

All reagents used in this study were purchased from Aladdin Chemicals and used without further purification. To prepare the Cu_2MoS_4 nanoparticles, 0.4 g of CuCl, 2.4 g of $(NH_4)_6Mo_7O_{24}$, and 2.231 g of $Na_2S{\cdot}9H_2O$ were mixed for 20 min by grinding them using a mortar and pestle. Further, the mixture was kept in a vacuum oven at 200°C for 3 h. The resulting brown-red product was washed using deionized water several times with the help of a centrifuge that was maintained at 10000 r/min for 10 min. Finally, the resulting product was vacuum-dried at 70°C for 6 h.

2.2. Photodegradation experiments

Various quantities (15, 30, and 50 mg) of the synthesized Cu_2MoS_4 samples were individually placed into an aqueous solution of MB (100 mL, 15 mg/L) in a 200-mL cylindrical quartz vessel that was surrounded by a water-circulating jacket to cool the sample. Before the lamp was activated, the solution was stirred in the dark for 2 h to ensure adsorption/desorption equilibrium between Cu_2MoS_4 and MB. A 300 W tungsten-halogen lamp (Chaohua brand) was used as the source of visible-light and was placed 15 cm away from the quartz vessel. The mixture was constantly stirred, and approximately 3 mL of the mixture was sampled at various time intervals during both the dark and illuminated phases. After centrifugation, the ultraviolet–visible spectroscopy (UV-vis) spectrum of the supernatant was recorded to monitor the degradation process.

2.3. Characterization

The synthesized products were characterized using X-ray diffraction (XRD) with Cu K_α radiation (λ = 0.154178 nm). The valence states were identified using high resolution X-ray photoelectron spectroscopy (XPS, Mg K_α radiation, and C 1s peak (284.6 eV)). Images of Cu_2MoS_4 nanoparticles were obtained using a field emission scanning electron microscope (FESEM, JEOL, JSM-6340F), which was operated at an accelerating voltage of 200 kV. The adsorption UV-vis spectrum was recorded using a Shimadzu UV-2550 spectrophotometer. The absorbance of the MB solution samples during the photodegradation experiments was analyzed using a UV-vis spectrophotometer (UV-722).

3. Results and discussion

The structural information of Cu_2MoS_4 nanoparticles was investigated using XRD and the results are depicted in Fig. 1(a). The main diffraction peaks at 2θ around 16.68°, 29.14°, 38.28°, and 48.79° can be attributed to the (001), (111), (201), and (202) planes of Cu_2MoS_4, respectively. The analytical results are in good agreement with the tetragonal structure of Cu_2MoS_4 having a $P\bar{4}2m$ symmetry, which is similar to the structure of Cu_2WS_4 [12]. The estimated lattice parameters of Cu_2MoS_4 were $a = b = 0.54268$ nm and $c = 0.52256$ nm, which is consistent with the parameters that were previously reported [18,22]. XPS was employed to confirm the valence states of the Cu_2MoS_4 nanoparticles. As depicted in Fig. 1(b), the binding energy values of Cu $2p_{3/2}$ and Cu $2p_{1/2}$ were located at 933.4 and 953.2 eV, respectively, with the peak splitting that is observed at 19.8 eV corresponding to the Cu(I) state [18]. The Mo $3d_{5/2}$ and Mo $3d_{3/2}$ peaks that were located at 229.1 and 232.1 eV, respectively, exhibit peak separation at 3.0 eV, indicative of Mo(VI) in Fig. 1(c) [18]. Fig. 1(d) depicts the binging energy peaks at 161.6 and 162.7 eV for S $2p_{3/2}$ and S $2p_{1/2}$, respectively, with the peak splitting that is observed to occur at 1.1 eV attributed to S(II) [18,22]. These binding energy values indicate that the product comprised Cu_2MoS_4 nanoparticles.

An FESEM image of Cu_2MoS_4 nanoparticles is shown in Fig. 2. This illustrates that the Cu_2MoS_4 microstructure is composed of a large number of small and thick nanoparticles possessing obvious aggregation. However, they are irregular in size, as depicted in Fig. 2(a). The chemical composition of the Cu_2MoS_4 nanoparticles was determined using an energy dispersive spectrometer, as illustrated in Fig. 2(b). The estimated chemical composition of the molar ratio of Cu:Mo:S was about 2:1:4. These results confirmed the successful synthesis of single-phase Cu_2MoS_4 nanoparticles.

The optical absorption properties of Cu_2MoS_4 nanoparticles were measured using UV-vis absorbance spectroscopy. The results depicted in Fig. 3(a) illustrate a broad absorption in the visible region. By extrapolating the linear region of the plot of $(\alpha h\nu)^2$ versus $h\nu$ (here α is the absorbance, h is the Plank's constant, and ν is the frequency), as depicted in the insert in Fig. 3(a), the band gap of Cu_2MoS_4 nanoparticles was estimated to be 1.66 eV. This result is in close proximity to the values that were reported in a previous study [16].

Based on strong visible-light absorption, the photocatalytic activity of Cu_2MoS_4 nanoparticles was investigated by measuring the degradation of MB ($C_{16}H_{18}ClN_3S$), as depicted in Fig. 3(b). The blank experiment depicted little MB degradation under visible light when catalyst was absent,

indicating that there was little contribution from the self-sensitization of MB. However, the dye quickly degraded at an irradiation time of 90 min when various quantities of Cu_2MoS_4 nanoparticles were added to the MB solution. The results indicate that Cu_2MoS_4 nanoparticles demonstrate good catalytic activity under visible light. Further comparative experiments were conducted to investigate the relationship between the degradation of MB and the quantity of Cu_2MoS_4 nanoparticles that was added to the solution, as depicted in Fig. 3(b). As the quantity of Cu_2MoS_4 nanoparticles that was added to the solution decreased, the degradation rate gradually decreased. This indicates that the proposed simple solid-phase synthesis process is an acceptable method for the preparation of low-cost Cu_2MoS_4 photocatalysts.

The stability of Cu_2MoS_4 nanoparticles for MB dye photodegradation was determined using XRD, as depicted in Fig. 4. The XRD patterns illustrate a comparative spectrum of the Cu_2MoS_4 nanoparticles, both before and after MB dye photodegradation treatment. No significant changes occur in the main peaks, showing the good structural stability of the Cu_2MoS_4 nanoparticles after MB dye photodegradation.

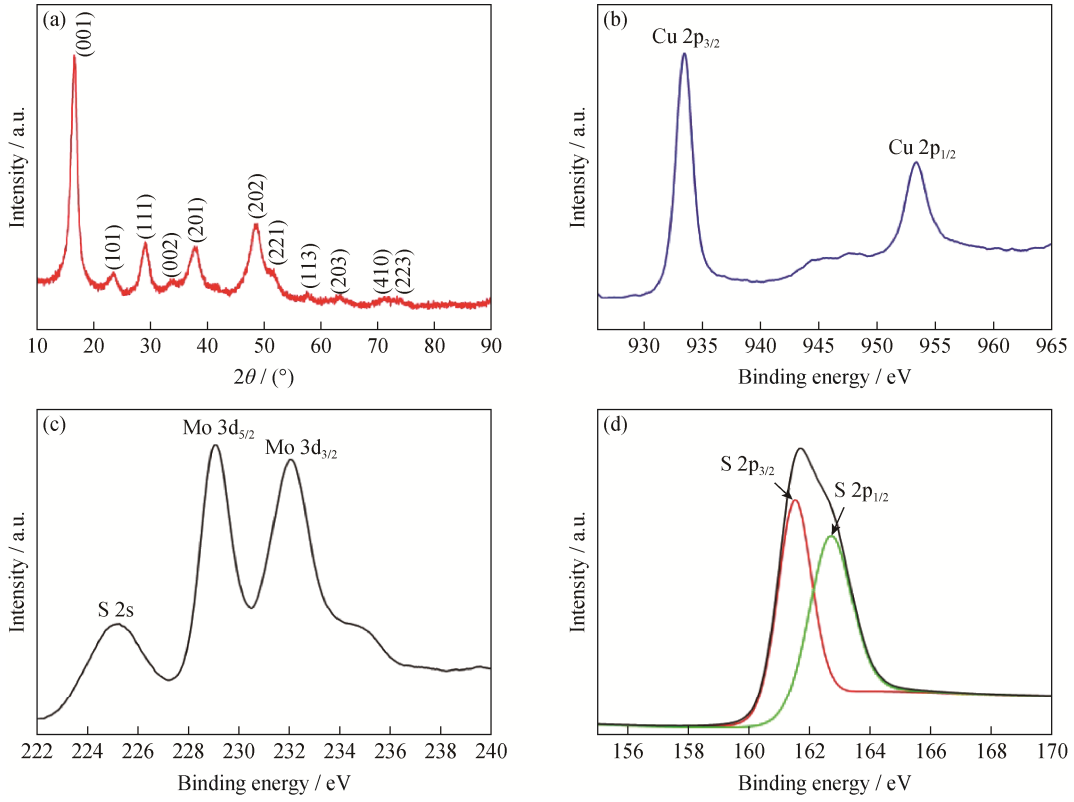

Fig. 1. XRD pattern (a), Cu 2p (b), Mo 3d and S 2s (c), and S 2p (d) XPS spectra of the synthesized Cu_2MoS_4 nanoparticles.

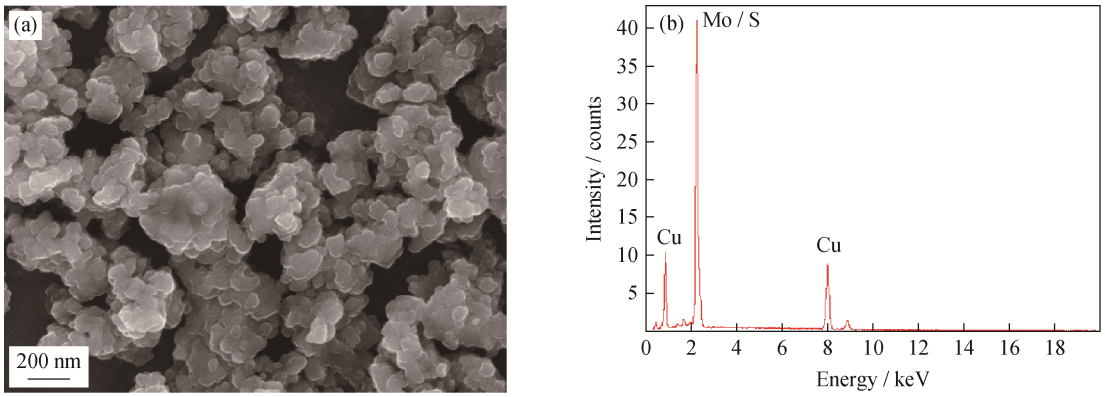

Fig. 2. FESEM image (a) and EDX spectrum (b) of as-synthesized Cu_2MoS_4.

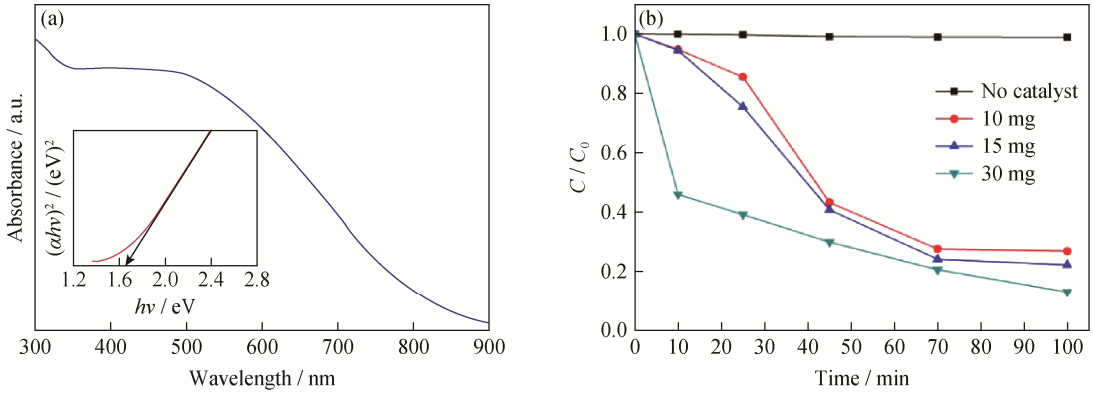

Fig. 3. UV-vis diffuse reflectance spectra of Cu_2MoS_4 nanoparticles (the insert depicts the corresponding plot of $(\alpha hv)^2$ versus hv) (a), and photocatalytic activities of Cu_2MoS_4 nanoparticles for MB degradation (C_0 is the initial concentration of MB and C is the concentration of MB after degradation) (b).

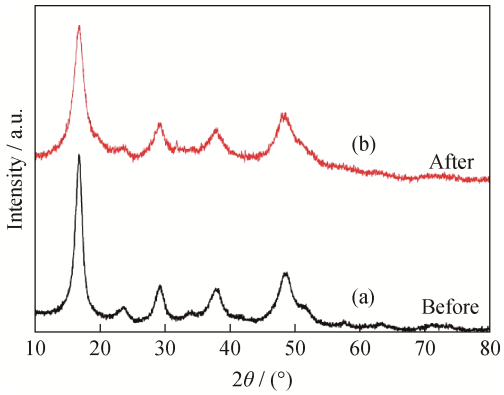

Fig. 4. XRD patterns of Cu_2MoS_4 nanoparticles before (a) and after (b) MB degradation.

4. Conclusions

To summarize, Cu_2MoS_4 nanoparticles were successfully prepared using a simple and environment-friendly solid-phase process, which was used for the first time, at 200°C for 3 h in air. The synthesized Cu_2MoS_4 nanoparticles possessed strong absorption properties in the visible-light region, and the band gap was determined to be 1.66 eV. Additionally, the Cu_2MoS_4 nanoparticles were used as a photocatalyst for the degradation of MB in an aqueous solution. Good photocatalytic activity in MB degradation was demonstrated by increasing the quantity of Cu_2MoS_4 nanoparticles. This study illustrates an innovative process for the quick and cheap mass-production of Cu_2MoS_4 photocatalysts.

Acknowledgement

The work was financially supported by the Fundamental Research Funds for the Central Universities (No. FRF-BD-15-004A).

References

[1] M. Chhowalla, H.S. Shin, G. Eda, L.J. Li, K.P. Loh, and H. Zhang, The chemistry of two-dimensional layered transition metal dichalcogenide nanosheets, *Nat. Chem.*, 5(2013), p. 263.

[2] F.C. Lei, Y.F. Sun, K.T. Liu, S. Gao, L. Liang, B.C. Pan, and Y. Xie, Oxygen vacancies confined in ultrathin indium oxide porous sheets for promoted visible-light water splitting, *J. Am. Chem. Soc.*, 136(2014), No. 19, p. 6826.

[3] M. Marchelek, E. Grabowska, T. Klimczuk, W. Lisowski, and A. Zaleska-Medynska, Various types of semiconductor photocatalysts modified by CdTe QDs and Pt NPs for toluene photooxidation in the gas phase under visible light, *Appl. Surf. Sci.*, 393(2017), p. 262.

[4] S.A. Ansari, Z. Khan, M.O. Ansari, and M.H. Cho, Earth-abundant stable elemental semiconductor red phosphorus-based hybrids for environmental remediation and energy storage applications, *RSC Adv.*, 6(2016), No. 50, p. 44616.

[5] S.K. Lakhera, R. Venkataramana, A. Watts, M. Anpo, and B. Neppolian, Facile synthesis of Fe_2O_3/Cu_2O nanocomposite and its visible light photocatalytic activity for the degradation of cationic dyes, *Res. Chem. Intermed.*, 43(2017), No. 9, p. 5091.

[6] S.G. Babu, R. Vinoth, B. Neppolian, D.D. Dionysiou, and M. Ashokkumar, Diffused sunlight driven highly synergistic pathway for complete mineralization of organic contaminants using reduced graphene oxide supported photocatalyst, *J. Hazard. Mater.*, 291(2015), p. 83.

[7] S.G. Babu, R. Vinoth, P.S. Narayana, D. Bahnemann, and B. Neppolian, Reduced graphene oxide wrapped Cu_2O supported on C_3N_4: An efficient visible light responsive semiconductor photocatalyst, *APL Mater.*, 3(2015), No. 10, art. No. 104415.

[8] S.K. Lakhera, A. Watts, H.Y. Hafeez, and B. Neppolian, Interparticle double charge transfer mechanism of heterojunc-

tion α-Fe_2O_3/Cu_2O mixed oxide catalysts and its visible light photocatalytic activity, *Catal. Today*, 300(2018), p. 58.

[9] Q. Jia, Y.C. Zhang, J. Li, Y. Chen, and B. Xu, Hydrothermal synthesis of Cu_2 WS_4 as a visible-light-activated photocatalyst in the reduction of aqueous Cr(VI), *Mater. Lett.*, 117(2014), No.7, p. 24.

[10] F. Ozel, E. Aslan, A. Sarilmaz, and P.I. Hatay, Hydrogen evolution catalyzed by Cu_2WS_4 at liquid–liquid interfaces, *ACS Appl. Mater. Interfaces*, 8(2016), No. 39, p. 25881.

[11] A.P. Tiwari, D. Kim, Y. Kim, O. Prakash, and H. Lee, Highly active and stable layered ternary transition metal chalcogenide for hydrogen evolution reaction, *Nano Energy*, 28(2016), p. 366.

[12] K. Zhang, W. Chen, Y. Lin, H. Chen, Y.A. Haleem, C. Wu, F. Ye, T.X. Wang, and L. Song, Self-assembly of ultrathin Cu_2MoS_4 nanobelts for highly efficient visible light-driven degradation of methyl orange, *Nanoscale*, 7(2015), No. 3, p. 17998.

[13] H.P. Chen, K. Zhang, W.X. Chen, I. Ali, P. Wu, D.B. Liu, and S. Li, Raman scattering of single crystal Cu_2MoS_4 nanosheet, *AIP Adv.*, 5(2015), No. 3, art. No. 037141.

[14] E.A. Pruss, B.S. Snyder, and A.M. Stacy, A new layered ternary sulfide: formation of Cu_2WS_4 by reaction of WS_4^{2-} and Cu^+ ions, *Angew. Chem. Int. Ed.*, 32(1993), No. 2, p. 256.

[15] C.J. Crossland, P.J. Hickey, and J.S.O. Evans, The synthesis and characterisation of Cu_2MX_4 (M= W or Mo; X = S, Se or S/Se) materials prepared by a solvothermal method, *J. Mater. Chem.*, 15(2005), No. 34, p. 3452.

[16] H.R. Liang and L.J. Guo, Synthesis, characterization and photocatalytic performances of Cu_2MoS_4, *Int. J. Hydrogen Energy*, 35(2010), No. 13, p. 7104.

[17] D.W. Jing, M.C. Liu, Q.Y. Chen, and L.J. Guo, Efficient photocatalytic hydrogen production under visible light over a novel W-based ternary chalcogenide photocatalyst prepared by a hydrothermal process, *Int. J. Hydrogen Energy*, 35(2010), No. 16, p. 8521.

[18] P.D. Tran, N. Mai, S.S. Pramana, A. Bhattacharjee, S.Y. Chiam, J. Fize, M.J. Field, V. Artero, L.H. Wong, J. Loo, and J. Barber, Copper molybdenum sulfide: a new efficient electrocatalyst for hydrogen production from water, *Energy Environ. Sci.*, 5(2012), No. 10, p. 8912.

[19] K. Zhang, W.X. Chen, Y. Wang, J. Li, H.P. Chen, Z.Y. Gong, S. Chang, F. Ye, T.X. Wang, W.S. Chu, C.W. Zou, and L. Song, Cube-like Cu_2MoS_4 photocatalysts for visible light-driven degradation of methyl orange, *AIP Adv.*, 5(2015), No. 7, art. No. 077130.

[20] B.B. Chen, D.K. Ma, Q.P. Ke, W. Chen, and S.M. Huang, Indented Cu_2MoS_4 nanosheets with enhanced electrocatalytic and photocatalytic activities realized through edge engineering, *Phys. Chem. Chem. Phys.*, 18(2016), No. 9, p. 6713.

[21] R.X. Ma, F. Yang, S.N. Li, X.Y. Zhang, X. Li, S.Y. Cheng, and Z.L. Liu, Fabrication of $Cu_2ZnSn(S,Se)_4$ (CZTSSe) absorber films based on solid-phase synthesis and blade coating processes, *Appl. Surf. Sci.*, 368(2016), p. 8.

[22] W.X. Chen, H.P. Chen, H.Z. Zhu, Q.Q. Gao, J. Luo, Y. Wang, S. Zhang, K. Zhang, C.G. Wang, Y.J. Xiong, Y.F. Wu, X.S. Zheng, W.S. Chu, L. Song, and Z.Y. Wu, Solvothermal synthesis of ternary Cu_2MoS_4 nanosheets: structural characterization at the atomic level, *Small*, 10(2014), No. 22, p. 4637.